Research Article | Vol. 26, No. 4 | 19 Feb 2018 | OPTICS EXPRESS 4605
Optics EXPRESS

Characterization of the stochastic time evolution of short-term average intercore crosstalk in multicore fibers with multiple interfering cores

TIAGO M. F. ALVES[1,*] AND ADOLFO V. T. CARTAXO,[1,2]

[1] *Instituto de Telecomunicações, 1049-001 Lisbon, Portugal*
[2] *ISCTE - Instituto Universitário de Lisboa, 1649-026 Lisbon, Portugal*
[*] *tiago.alves@lx.it.pt*

Abstract: A theoretical model for the stochastic time evolution of the intercore crosstalk (ICXT) in homogeneous weakly-coupled multicore fibers (MCF) with multiple interfering cores is proposed and validated experimentally. The model relies on the introduction of non-stationary time varying random phase shifts at every center point between the phase matching points of the MCF where the difference of the effective refractive indexes of the core of the originating signal and the core suffering from ICXT is zero. Closed form-expressions for the autocovariance of the short-term average ICXT (STAXT) with stationary and non-stationary phase shift models in MCFs with multiple excited cores are derived and validated by comparison with experimental results. These expressions enable estimating the decorrelation time of the STAXT generated by multiple interfering cores from the decorrelation times of the STAXT generated by each pair of cores. The proposed model and the ICXT measurements taken continuously over more than 150 hours show that the decorrelation time of the STAXT generated by multiple interfering cores exceeds the one obtained for the pair of cores with shorter decorrelation time. The proposed model is increasingly important to simulate and design MCF-based systems where the ICXT dynamics must be properly accounted for to develop efficient ICXT-tolerant techniques.

OCIS codes: (060.2330) Fiber optics communications; (060.2270) Fiber characterization.

References and links

1. H. Takahashi, K. Igarashi, and T. Tsuritani, "Long-haul transmission using multicore fibers," in Optical Fiber Communication Conference, OSA Technical Digest (Optical Society of America, 2014), paper Tu2J.2.
2. J. Galvé, I. Gasulla, S. Sales, and J. Capmany, "Reconfigurable radio access networks using multicore fibers," J. Quantum Electron. **52**(1), 0600507 (2016).
3. Z. Feng, B. Li, M. Tang, L. Gan, R. Wang, R. Lin, Z. Xu, S. Fu, L. Deng, W. Tong, S. Long, L. Zhang, H. Zhou, R. Zhang, S. Liu, and P. Shum, "Multicore-fiber-enabled WSDM optical access network with centralized carrier delivery and RSOA-based adaptive modulation," Photon. J. **7**(4), 7201309 (2015).
4. D. Butler, M. Li, S. Li, Y. Geng, R. Khrapko, R. Modavis, V. Nazarov, and A. Koklyushkin, "Space division multiplexing in short reach optical interconnects," J. Lightw. Technol. DOI 10.1109/JLT.2016.2619981 (2017).
5. Y. Amma, Y. Sasaki, K. Takenaga, S. Matsuo, J. Tu, K. Saitoh, M. Koshiba, T. Morioka, and Y. Miyamoto, "High-density multicore fiber with heterogeneous core arrangement," in Optical Fiber Communication Conference, OSA Technical Digest (Optical Society of America, 2015), paper Th4C.4.
6. A. Cartaxo and T. Alves, "Discrete changes model of inter-core crosstalk of real homogeneous multi-core fibers," J. Lightw. Technol. DOI 10.1109/JLT.2017.2652067 (2017).
7. B. Puttnam, R. Luís, E. Agrell, G. Rademacher, J. Sakaguchi, W. Klaus, G. Saridis, Y. Awaji, and N. Wada, "High capacity transmission systems using homogeneous multi-core fibers," J. Lightw. Technol. **35**(6), 1157–1167 (2017).
8. B. Puttnam, R. Luís, T. Eriksson, W. Klaus, J. Mendinueta, Y. Awaji, and N. Wada, "Impact of intercore crosstalk on the transmission distance of QAM formats in multicore fibers," Photon. J. **8**(2), 0601109 (2016).
9. T. Nagashima, O. Shimakawa, T. Sasaki, and E. Sasaoka, "Crosstalk variation of multi-core fibre due to fibre bend," in European Conference on Optical Communications (ECOC), (2010), paper We.8.F.6.
10. J. Fini, B. Zhu, T. Taunay, and M. Yan, "Statistics of crosstalk in bent multicore fibers," Opt. Express **18**, 15122-15129 (2010).
11. M. Koshiba, K. Saitoh, K. Takenaga, and S. Matsuo, "Analytical expression of average power-coupling coefficients for estimating intercore crosstalk in multicore fibers," Photon. J. **4**(5), 1987–1995 (2012).

#313711 https://doi.org/10.1364/OE.26.004605
Journal © 2018 Received 16 Nov 2017; revised 12 Jan 2018; accepted 16 Jan 2018; published 13 Feb 2018

Optics EXPRESS

12. T. Hayashi, T. Taru, O. Shimakawa, T. Sasaki, and E. Sasaoka, "Design and fabrication of ultra-low crosstalk and low-loss multi-core fiber," Opt. Express **19**(17), 16576–16592 (2011).
13. A. Cartaxo, R. Luís, B. Puttnam, T. Hayashi, Y. Awaji, and N. Wada, "Dispersion impact on the crosstalk amplitude response of homogeneous multi-core fibers," Photon. Technol. Lett. **28**(17), 1858–1861 (2016).
14. R. Soeiro, T. Alves, and A. Cartaxo, "Dual polarization discrete changes model of inter-core crosstalk in multi-core fibers," Photon. Technol. Lett. **29**(16), 1395-1398 (2017).
15. R. Luís, B. Puttnam, A. Cartaxo, W. Klaus, J. Mendinueta, Y. Awaji, N. Wada, T. Nakanishi, T. Hayashi, and T. Sasaki, "Time and modulation frequency dependence of crosstalk in homogeneous multi-core fibers," J. Lightw. Technol. **34**(2), 441–447 (2016).
16. T. Alves, R. Luís, B. Puttnam, A. Cartaxo, Y. Awaji, and N. Wada, "Performance of adaptive DD-OFDM multicore fiber links and its relation with intercore crosstalk," Opt. Express **25**(13), 16017–16027 (2017).
17. G. Rademacher, B. Puttnam, R. Luís, Y. Awaji, and N. Wada, "Time-dependent inter-core crosstalk between multiple cores of a homogeneous multi-core fiber," in Proceedings of Asia Communications and Photonics Conference (ACPC), paper AF1D.2 (2016).
18. G. Rademacher, B. Puttnam, R. Luís, Y. Awaji, and N. Wada, "Time-dependent crosstalk from multiple cores in a homogeneous multi-core fiber," in Optical Fiber Communication Conference, OSA Technical Digest (Optical Society of America, 2016), paper Th1H.3.
19. W. Klaus, B. Puttnam, R. Luis, J. Sakaguchi, J. Mendinueta, Y. Awaji, and N. Wada, "Advanced space division multiplexing technologies for optical networks," J. Opt. Commun. Netw. **9**(4), C1-C11 (2017).
20. A. Macho, M. Morant, and R. Llorente, "Experimental evaluation of nonlinear crosstalk in multi-core fiber," Opt. Express **32**, 18712-18720 (2015).
21. J. Pedro, R. Luís, B. Puttnam, Y. Awaji, N. Wada, and A. Cartaxo, "Experimental assessment of the time-varying impact of multi-core fiber crosstalk on a SSB-OFDM Signal," in Proceedings of Photonics in Switching (PS), 166–168 (2015).
22. A. Cartaxo, T. Alves, B. Puttnam, R. Luís, Y. Awaji, and N. Wada, "DD-OFDM multicore fiber systems impaired by intercore crosstalk and laser phase noise," in Proceedings of International Conference on Transparent Optical Networks (ICTON), paper Tu.D1.1 (2017).
23. T. Alves and A. Cartaxo, "Characterization of ICXT in DD-OFDM MCF-based systems," in Proceedings of European Conference on Optical Communications (ECOC), paper P2.SC6.29 (2017).
24. G. Rademacher, R. Luís, B. Puttnam, Y. Awaji, and N. Wada, "Performance fluctuations in direct detection multi-core fiber transmission systems," in Proceedings of European Conference on Optical Communications (ECOC), paper P2.SC6.16 (2017).
25. T. Alves, A. Cartaxo, R. Luís, B. Puttnam, Y. Awaji, and N. Wada, "Adaptive loading with extended memory to relax the impact of the phase noise-impaired ICXT in DD-OFDM MCF-based systems," in Proceedings of International Conference on Transparent Optical Networks (ICTON), paper Tu.D1.2 (2017).
26. G. Rademacher, R. Luís, B. Puttnam, Y. Awaji, and N. Wada, "Crosstalk dynamics in multi-core fibers," Opt. Express **25**(10), 12020–12028 (2017).
27. T. Alves, A. Cartaxo, R. Luís, B. Puttnam, Y. Awaji, and N. Wada, "Intercore crosstalk in direct-detection homogeneous multicore fiber systems impaired by laser phase noise," Opt. Express **25**(23), 29417–29431 (2017).
28. P. Winzer, A. Gnauck, A. Konczykowska, F. Jorge, and J. Dupuy, "Penalties from in-band crosstalk for advanced optical modulation formats," in Proceedings of European Conference on Optical Communications (ECOC), paper Tu.5.B.7 (2011).
29. T. Alves and A. Cartaxo, "Inter-core crosstalk in homogeneous multi-core fibers: theoretical characterization of stochastic time evolution," J. Lightw. Technol. **35**(21), 4613–4623 (2017).
30. J. Franz and V. Jain, *Optical Communications: Components and Systems* (Alpha Science International Limited, reprint in 2008).
31. T. Hayashi, T. Nagashima, O. Shimakawa, T. Sasaki, and E. Sasaoka, "Crosstalk variation of multi-core fibre due to fibre bend," in Proceedings of European Conference on Optical Communications (ECOC), paper We.8.F.6. (2010).

1. Introduction

Multicore fiber (MCF) technology is a powerful candidate to overcome the capacity crunch foreseen for the near future in different optical networks. MCF-based systems have been recently proposed for long-haul, radio-over-fiber, access networks, or data center connectivity [1–4]. In these systems, different cores of each fiber are used for simultaneous transmission of information signals. MCFs are commonly classified into homogeneous and heterogeneous fibers. Homogeneous MCFs, in which the physical properties of different cores are nearly identical, are characterized by similar signal propagation times along the different cores and non-negligible intercore crosstalk (ICXT) levels that increase with the fiber reach [5–7]. Heterogeneous MCFs, with cores with significantly different refraction indexes or radii, are generally characterized by

Optics EXPRESS

low ICXT, higher core-count and different propagation times between cores [7, 8].

The ICXT generated in weakly-coupled homogeneous MCFs is characterized by a random variation along the longitudinal direction of the fiber [9–11]. A theoretical model that suitably describes this random ICXT behavior in weakly-coupled homogeneous MCFs has been proposed [6, 12–14]. The model is based on the introduction of random phase shifts at every center point between the phase matching points (PMPs) of the MCF where the difference of the effective refractive indexes of the core of the originating signal and the core suffering from ICXT is zero [9, 12]. Recently, remarkable fluctuations of the short term average crosstalk (STAXT) over time were shown [15–20]. The STAXT is defined as the average ICXT power measured, in the absence of signal modulation, by a power meter during a short period of time [15]. Experimental observations have shown that the photodetected ICXT in weakly-coupled homogeneous MCFs varies randomly also over time and frequency [15, 16, 21–25].

Previous works showed that the impact of the ICXT on the performance is significantly dependent on the modulation format, data-rate, temporal skew between cores, kind of optical receiver, etc., employed in the MCF system [8, 26, 27]. In [28], a maximum average crosstalk level of -32 dB to maintain the optical signal-to-noise-ratio (OSNR) penalty below 1 dB for systems using 64 quadrature amplitude modulation (QAM) format was shown. In [8], experimental results suggest that the ICXT can significantly limit the transmission distance of 25 GBd polarization division multiplexing (PDM) systems using 4-QAM, 16-QAM or 64-QAM modulation formats when the ICXT levels exceed 40 dB/100 km. More recently, it was concluded that MCF-based systems employing carrier free signals and large temporal skews between cores exhibit nearly constant ICXT power over time [26]. Contrarily, direct detection (DD) MCF systems using carrier supported signals are impaired by ICXT power that may fluctuate significantly over time [26, 27]. Thus, short-reach access networks, data-centers or other systems, where MCFs with high core count and low-cost DD receivers are preferable to maximize the spatial information density at a reduced cost, may be particularly affected by the dynamic behavior of ICXT over time and require a performance margin to operate adequately [26].

Despite the need of understanding in detail the time properties of the ICXT fluctuations to design new MCF systems with low outage probability, only very few works have addressed the theoretical analysis of this stochastic ICXT effect. In [29], the random time nature of the ICXT and STAXT in weakly-coupled homogeneous MCFs have been theoretically modeled by including a stochastic time variation in each phase shift. A Brownian motion has been proposed to model the time evolution of the phase shifts, and closed form expressions for the autocorrelation and autocovariance functions of the STAXT have been proposed. With this model, derived considering only one interfering core, simulation of the time varying nature of the ICXT in MCFs can be performed. In [17], the time varying nature of the STAXT is also modeled by introducing a stochastic time variation in each phase shift. However, the time evolution of the phase shift is not modeled analytically. Instead, the faster or slower variation of the time varying STAXT observed experimentally for different pairs of cores is obtained by qualitatively changing the number of random perturbations applied to the original phase shift in a given time interval. As a consequence, it is not straightforward to replicate the experimental results through simulation.

In this work, a theoretical model that characterizes the stochastic time evolution of the ICXT in weakly-coupled homogeneous MCFs with multiple excited cores is proposed. Closed form-expressions for the autocovariance of the STAXT with stationary and non-stationary phase shift models are derived and compared with simulation and experimental results. In addition, the decorrelation time of the STAXT generated by single or multiple interfering cores is evaluated from the proposed model and compared with experimental measurements.

The remainder of the paper is organized as follows. Section 2 presents the theory of the proposed ICXT model. Section 3 describes the system parameters and the setup employed in experiments and in the simulation analysis. In section 4, the autocorrelation and autocovariance of

Optics EXPRESS

the STAXT obtained with the proposed ICXT model are validated by simulation. The validation is performed for multiple interfering cores and considering MCFs with different decorrelation times between pairs of cores. Section 5 presents the experimental results of the STAXT and decorrelation time of each pair of cores of the MCF used in the lab. From these results, the parameters required by the theoretical model to evaluate the autocovariance of the STAXT are estimated and the autocovariance of the STAXT evaluated from the proposed model with multiple interfering cores is validated. The conclusion of the work is presented in Section 6.

2. Theory

The dual polarization ICXT model proposed in [14, 29] considers only two MCF cores, namely, the interfering and the test core. In this section, that ICXT model is generalized to account for a MCF with N_c cores, with N_c-1 cores excited at the transmitter side and the other core acting as the test core. Analytical expressions for the autocovariance function of the STAXT considering the time evolution of the phase shifts described by a stationary or a non-stationary random process are also proposed.

2.1. ICXT field in a MCF with multiple excited cores

Due to the weakly-coupled regime of the homogeneous MCFs considered in this work, we can assume that the ICXT field at the output of a MCF with multiple cores excited at the transmitter side results from adding the independent ICXT contributions generated by each one of the excited cores. Considering identical loss coefficient in the different cores of the MCF, the slowly varying complex amplitude of the electric field of the interfered core n at the MCF output normalized by the core loss, $\mathbf{E}_n(L,t) = [E_{n,x}(L,t)\ \ E_{n,y}(L,t)]^T$, can be written from the dual polarization ICXT model proposed in [14, 29] as

$$\mathbf{E}_n(L,t) = -j \sum_{\substack{m=1,\\ m\neq n}}^{N_c} \frac{\overline{K}_{n,m}}{\sqrt{2}} \sum_{k=1}^{N_p} \begin{bmatrix} \sqrt{\zeta_m} v_{1,n,m}^{(k)}(t) & \sqrt{1-\zeta_m} v_{2,n,m}^{(k)}(t) \\ \sqrt{\zeta_m} v_{3,n,m}^{(k)}(t) & \sqrt{1-\zeta_m} v_{4,n,m}^{(k)}(t) \end{bmatrix} \begin{bmatrix} \overline{F}_{n,m}^{(k)}\left(0, t-\overline{\xi}_{n,m}^{(k)}\right) \\ \overline{F}_{n,m}^{(k)}\left(0, t-\overline{\xi}_{n,m}^{(k)}\right) \end{bmatrix} \tag{1}$$

where L is the MCF length, t is the time, N_c is the number of cores of the MCF, N_p is the number of PMPs, $\zeta_m \in [0,1]$ is the level of power splitting between the polarization directions at the input of the m-th interfering core, $\overline{K}_{n,m}$ is the discrete coupling coefficient evaluated from the average of the intercore coupling coefficients (between cores n and m) of the two orthogonal polarization directions $\mathbf{u_x}$ and $\mathbf{u_y}$, $\overline{\kappa}_{n,m}$=0.5 $\left(\kappa_{n,m,x} + \kappa_{n,m,y}\right)$, and

$$v_{i,n,m}^{(k)}(t) = \exp\left[-j(\Phi_{i,m}^{(k)}(t) + \overline{\phi}_{n,m}^{(k)})\right], \qquad 1 \le i \le 4 \tag{2}$$

$$\overline{F}_{n,m}^{(k)}(0,t) = \mathcal{F}^{-1}\left[\tilde{E}_m(0,\omega) \exp\left(-j\overline{\eta}_{n,m}^{(k)}\omega^2\right)\right] \tag{3}$$

$$\overline{\phi}_{n,m}^{(k)} = \overline{\beta}_{n,0}\left(L - z_m^{(k)}\right) + \overline{\beta}_{m,0} z_m^{(k)} \qquad \overline{\xi}_{n,m}^{(k)} = \overline{\beta}_{n,1}\left(L - z_m^{(k)}\right) + \overline{\beta}_{m,1} z_m^{(k)} \tag{4}$$

$$\overline{\eta}_{n,m}^{(k)} = 0.5\left[\overline{\beta}_{n,2}\left(L - z_m^{(k)}\right) + \overline{\beta}_{m,2} z_m^{(k)}\right] \tag{5}$$

where ω is the angular frequency, $\mathcal{F}^{-1}$ is the inverse Fourier transform operator, $\tilde{E}_m(0,\omega)$ is the Fourier transform of the slowly varying complex amplitude of the electric field of the m-th

Optics EXPRESS

interfering core at the MCF input and $z_m^{(k)}$ is the longitudinal coordinate of the MCF corresponding to the k-th center point between consecutive PMPs of core m. $\overline{\beta}_{q,i}$ (with $i = 1$ or $i = 2$) is the average of the i-th order derivative of the intrinsic propagation constant of core q of the two polarizations with respect to angular frequency and $\Phi_{i,m}^{(k)}(t)$ are independent random processes that represent the contributions of the time varying nature of the phase shift associated with each PMP of the m-th interfering core to the Jones vector of the ICXT field. The functions $v_{i,n,m}^{(k)}(t)$ represent the coupling between the polarization directions [14, 29]. The instantaneous ICXT power in the dual polarization scheme is given by $p(t) = |E_{n,x}(L,t)|^2 + |E_{n,y}(L,t)|^2$.

In [29], the time varying phase shifts of the ICXT model associated with each PMP are assumed stationary and modeled by independent Brownian motions. Here, the statistical characterization of the time varying of the phase shift associated with each PMP of each interfering core in MCFs with multiple excited cores is developed considering an independent non-stationary Wiener process for each time varying phase shift. These two different statistical characterizations of the phase shifts are compared with experimental results and discussion about which model is more suitable to provide good description of the time varying nature of the ICXT is accomplished.

2.1.1. Non-stationary phase shift model

The non-stationary model of the phase shifts considered in this work is based on the Wiener process that is commonly used to characterize the laser phase noise in optical fiber communication systems. The non-stationary model for each phase shift associated with each PMP of each interfering core can be written as:

$$\Phi_{i,m}^{(k)}(t) = 2\pi \int_0^t \mu_{i,m}^{(k)}(\tau)\, d\tau \qquad t > 0 \tag{6}$$

where $\mu_{i,m}^{(k)}(\tau)$ is the instantaneous frequency associated with the k-th PMP of the m-th interfering core. In each PMP, $\mu_{i,m}^{(k)}(\tau)$ is a zero mean white Gaussian noise process with double sided power spectral density (PSD) given by $S_{\mu,m}$=$K_{\Phi_m}/(2\pi)^2$, where K_{Φ_m} is a parameter associated with the decorrelation time of the STAXT generated by core m in core n. With the model of Eq. (6), each phase shift is a non-stationary Gaussian process with zero mean and variance given by $\sigma^2_{\Phi_{i,m}^{(k)}}(t)$=$(2\pi)^2 S_{\mu,m} t$. As the phase shifts of different cores and the phase shifts of the same core but in different PMPs are uncorrelated, we also have

$$\begin{aligned} R_{ns,m_1,m_2,k_1,k_2}(\tau) &= \mathrm{E}\left\{\exp\left[\pm j\left(\Phi_{i,m_1}^{(k_1)}(t) - \Phi_{i,m_2}^{(k_2)}(t+\tau)\right)\right]\right\} = \\ &= \begin{cases} \exp\left(-0.5 K_{\Phi_m}|\tau|\right) & \text{for } m_1{=}m_2 \text{ and } k_1{=}k_2 \\ \mathrm{E}\left\{\exp\left[\pm j\Phi_{i,m_1}^{(k_1)}(t)\right]\right\}\mathrm{E}\left\{\exp\left[\mp j\Phi_{i,m_2}^{(k_2)}(t+\tau)\right]\right\} = 0 & \text{for } m_1 \neq m_2 \text{ or } k_1 \neq k_2 \end{cases} \end{aligned} \tag{7}$$

where τ is the time lag. In Eq. (7), we considered $\mathrm{E}\left\{\exp\left[\pm j\Phi_{i,m}^{(k)}(t)\right]\right\} = 0$ because $\Phi_{i,m}^{(k)}(t)$ is uniformly distributed between 0 and 2π. The autocorrelation of the non-stationary phase shifts in the same PMP of the same core is given on page 72 in [30]. In the following, for the sake of notation simplicity, $R_{ns,m_1,m_2,k_1,k_2}(\tau)$ is referred to simply as $R_{ns,m}(\tau)$.

2.2. Autocovariance of the STAXT in MCFs with multiple excited cores

In this section, the autocovariance of the STAXT in MCFs with multiple excited cores is derived from the dual polarization ICXT model considering the non-stationary phase shift model proposed in this work and the stationary model presented in [29].

The evaluation of the STAXT is performed using a constant signal (absence of signal modulation) at the input of the interfering cores. Under this condition, the slowly varying complex

Optics EXPRESS

amplitude of the electric field of the interfered core n at the MCF output in each polarization direction is given by

$$E_{n,x}(L,t) = -j \sum_{\substack{m=1,\\ m\neq n}}^{N_c} \frac{\sqrt{p_{i,m}}\overline{K}_{n,m}}{\sqrt{2}} \sum_{k=1}^{N_p} \left(\sqrt{\zeta_m} v_{1,n,m}^{(k)}(t) + \sqrt{1-\zeta_m} v_{2,n,m}^{(k)}(t) \right) \tag{8}$$

$$E_{n,y}(L,t) = -j \sum_{\substack{m=1,\\ m\neq n}}^{N_c} \frac{\sqrt{p_{i,m}}\overline{K}_{n,m}}{\sqrt{2}} \sum_{k=1}^{N_p} \left(\sqrt{\zeta_m} v_{3,n,m}^{(k)}(t) + \sqrt{1-\zeta_m} v_{4,n,m}^{(k)}(t) \right) \tag{9}$$

where $p_{i,m}$ is the power at the input of the interfering core m, i. e., after the fan-in.

Let us consider that the STAXT is measured in a time interval, T, much smaller than the decorrelation time of the STAXT (in [15], T=100 ms and the decorrelation time of the STAXT is of the order of a few minutes). Considering that the instantaneous power of the ICXT is nearly constant within this time interval, the STAXT of core n can be written as

$$STAXT_n(t) = \frac{1}{T} \int_t^{t+T} p(\tau) d\tau \approx p(t) \tag{10}$$

Using Eq. 8 and Eq. 9, the mean power of the STAXT of core n evaluated from Eq. (10) is $\mathrm{E}[p(t)]=N_p \sum_{\substack{m=1,\\ m\neq n}}^{N_c} p_{i,m}|\overline{K}_{n,m}|^2$, where $\mathrm{E}[x]$ is the expected value of x. Considering the ICXT field in the two polarization directions characterized by phase shifts with identical STAXT decorrelation times, the autocorrelation of the STAXT of core n is given by:

$$R_{STAXT,n}(\tau) = \mathrm{E}\left[p(t)\, p(t+\tau)\right] = R_{STAXT,n,x}(\tau) + R_{STAXT,n,y}(\tau) + R_{STAXT,n,xy}(\tau) \tag{11}$$

where $R_{STAXT,n,x}(\tau)$ and $R_{STAXT,n,y}(\tau)$ are contributions of the autocorrelation of the STAXT originated from the power injected at the input of the m-th interfering core in polarizations $\mathbf{u_x}$ and $\mathbf{u_y}$, respectively, and $R_{STAXT,n,xy}(\tau)$ is a contribution obtained from the product of powers injected in different polarizations. These contributions are given by

$$\begin{aligned} R_{STAXT,n,x}(\tau) = {} & \frac{1}{2} \sum_{\substack{m_1=1,\\ m_1\neq n}}^{N_c} \sum_{\substack{m_2=1,\\ m_2\neq n}}^{N_c} \sum_{\substack{m_3=1,\\ m_3\neq n}}^{N_c} \sum_{\substack{m_4=1,\\ m_4\neq n}}^{N_c} \sqrt{p_{i,m_1} p_{i,m_2} p_{i,m_3} p_{i,m_4}} \overline{K}_{n,m_1} \overline{K}_{n,m_2}^{*} \overline{K}_{n,m_3} \overline{K}_{n,m_4}^{*} \times \\ & \times \sum_{k_1=1}^{N_p} \sum_{k_2=1}^{N_p} \sum_{k_3=1}^{N_p} \sum_{k_4=1}^{N_p} \exp\left[-j(\phi_{n,m_1}^{(k_1)} - \phi_{n,m_2}^{(k_2)} + \phi_{n,m_3}^{(k_3)} - \phi_{n,m_4}^{(k_4)})\right] \times \\ & \times \sqrt{\zeta_{m_1}\zeta_{m_2}\zeta_{m_3}\zeta_{m_4}} \left\{ \mathrm{E}\left[\exp\left\{-j\left(\Phi_{1,m_1}^{(k_1)}(t) - \Phi_{1,m_2}^{(k_2)}(t) + \Phi_{1,m_3}^{(k_3)}(t+\tau) - \Phi_{1,m_4}^{(k_4)}(t+\tau)\right)\right\}\right] + \right. \\ & \left. + \mathrm{E}\left[\exp\left\{-j\left(\Phi_{1,m_1}^{(k_1)}(t) - \Phi_{1,m_2}^{(k_2)}(t) + \Phi_{3,m_3}^{(k_3)}(t+\tau) - \Phi_{3,m_4}^{(k_4)}(t+\tau)\right)\right\}\right]\right\} \end{aligned} \tag{12}$$

$$\begin{aligned} R_{STAXT,n,y}(\tau) = {} & \frac{1}{2} \sum_{\substack{m_1=1,\\ m_1\neq n}}^{N_c} \sum_{\substack{m_2=1,\\ m_2\neq n}}^{N_c} \sum_{\substack{m_3=1,\\ m_3\neq n}}^{N_c} \sum_{\substack{m_4=1,\\ m_4\neq n}}^{N_c} \sqrt{p_{i,m_1} p_{i,m_2} p_{i,m_3} p_{i,m_4}} \overline{K}_{n,m_1} \overline{K}_{n,m_2}^{*} \overline{K}_{n,m_3} \overline{K}_{n,m_4}^{*} \times \\ & \times \sum_{k_1=1}^{N_p} \sum_{k_2=1}^{N_p} \sum_{k_3=1}^{N_p} \sum_{k_4=1}^{N_p} \left\{ \exp\left[-j(\phi_{n,m_1}^{(k_1)} - \phi_{n,m_2}^{(k_2)} + \phi_{n,m_3}^{(k_3)} - \phi_{n,m_4}^{(k_4)})\right] \sqrt{(1-\zeta_{m_1})(1-\zeta_{m_2})(1-\zeta_{m_3})} \times \right. \\ & \times \sqrt{(1-\zeta_{m_4})} \left\{ \mathrm{E}\left[\exp\left\{-j\left(\Phi_{2,m_1}^{(k_1)}(t) - \Phi_{2,m_2}^{(k_2)}(t) + \Phi_{2,m_3}^{(k_3)}(t+\tau) - \Phi_{2,m_4}^{(k_4)}(t+\tau)\right)\right\}\right] + \right. \\ & \left. \left. + \mathrm{E}\left[\exp\left\{-j\left(\Phi_{2,m_1}^{(k_1)}(t) - \Phi_{2,m_2}^{(k_2)}(t) + \Phi_{4,m_3}^{(k_3)}(t+\tau) - \Phi_{4,m_4}^{(k_4)}(t+\tau)\right)\right\}\right]\right\}\right\} \end{aligned} \tag{13}$$

Optics EXPRESS

$$R_{STAXT,n,xy}(\tau) = \frac{1}{2}\sum_{\substack{m_1=1,\\ m_1\neq n}}^{N_c}\sum_{\substack{m_2=1,\\ m_2\neq n}}^{N_c}\sum_{\substack{m_3=1,\\ m_3\neq n}}^{N_c}\sum_{\substack{m_4=1,\\ m_4\neq n}}^{N_c}\sqrt{p_{i,m_1}p_{i,m_2}p_{i,m_3}p_{i,m_4}}\overline{K}_{n,m_1}\overline{K}^{*}_{n,m_2}\overline{K}_{n,m_3}\overline{K}^{*}_{n,m_4}\times$$
$$\times\sum_{k_1=1}^{N_p}\sum_{k_2=1}^{N_p}\sum_{k_3=1}^{N_p}\sum_{k_4=1}^{N_p}\exp\left[-j(\phi^{(k_1)}_{n,m_1}-\phi^{(k_2)}_{n,m_2}+\phi^{(k_3)}_{n,m_3}-\phi^{(k_4)}_{n,m_4})\right]\times$$
$$\times\left\{\sqrt{\zeta_{m_1}(1-\zeta_{m_2})\zeta_{m_3}(1-\zeta_{m_4})}\times\right.$$
$$\times\,\mathrm{E}\left[\exp\left\{-j\left(\Phi^{(k_1)}_{1,m_1}(t)-\Phi^{(k_2)}_{2,m_2}(t)+\Phi^{(k_3)}_{1,m_3}(t+\tau)-\Phi^{(k_4)}_{2,m_4}(t+\tau)\right)\right\}\right]+$$
$$+\sqrt{(1-\zeta_{m_1})\zeta_{m_2}(1-\zeta_{m_3})\zeta_{m_4}}\times$$
$$\times\,\mathrm{E}\left[\exp\left\{-j\left(\Phi^{(k_1)}_{2,m_1}(t)-\Phi^{(k_2)}_{1,m_2}(t)+\Phi^{(k_3)}_{2,m_3}(t+\tau)-\Phi^{(k_4)}_{1,m_4}(t+\tau)\right)\right\}\right]+$$
$$+\sqrt{\zeta_{m_1}\zeta_{m_2}(1-\zeta_{m_3})(1-\zeta_{m_4})}\times$$
$$\times\,\mathrm{E}\left[\exp\left\{-j\left(\Phi^{(k_1)}_{1,m_1}(t)-\Phi^{(k_2)}_{1,m_2}(t)+\Phi^{(k_3)}_{2,m_3}(t+\tau)-\Phi^{(k_4)}_{2,m_4}(t+\tau)\right)\right\}\right]+$$
$$+\sqrt{\zeta_{m_1}\zeta_{m_2}(1-\zeta_{m_3})(1-\zeta_{m_4})}\times$$
$$\times\,\mathrm{E}\left[\exp\left\{-j\left(\Phi^{(k_1)}_{1,m_1}(t)-\Phi^{(k_2)}_{1,m_2}(t)+\Phi^{(k_3)}_{4,m_3}(t+\tau)-\Phi^{(k_4)}_{4,m_4}(t+\tau)\right)\right\}\right]+$$
$$+\sqrt{\zeta_{m_1}(1-\zeta_{m_2})(1-\zeta_{m_3})\zeta_{m_4}}\times$$
$$\times\,\mathrm{E}\left[\exp\left\{-j\left(\Phi^{(k_1)}_{1,m_1}(t)-\Phi^{(k_2)}_{2,m_2}(t)+\Phi^{(k_3)}_{2,m_3}(t+\tau)-\Phi^{(k_4)}_{1,m_4}(t+\tau)\right)\right\}\right]+$$
$$+\sqrt{(1-\zeta_{m_1})\zeta_{m_2}\zeta_{m_3}(1-\zeta_{m_4})}\times$$
$$\times\,\mathrm{E}\left[\exp\left\{-j\left(\Phi^{(k_1)}_{2,m_1}(t)-\Phi^{(k_2)}_{1,m_2}(t)+\Phi^{(k_3)}_{1,m_3}(t+\tau)-\Phi^{(k_4)}_{2,m_4}(t+\tau)\right)\right\}\right]+$$
$$+\sqrt{(1-\zeta_{m_1})(1-\zeta_{m_2})\zeta_{m_3}\zeta_{m_4}}\times$$
$$\times\,\mathrm{E}\left[\exp\left\{-j\left(\Phi^{(k_1)}_{2,m_1}(t)-\Phi^{(k_2)}_{2,m_2}(t)+\Phi^{(k_3)}_{1,m_3}(t+\tau)-\Phi^{(k_4)}_{1,m_4}(t+\tau)\right)\right\}\right]+$$
$$+\sqrt{(1-\zeta_{m_1})(1-\zeta_{m_2})\zeta_{m_3}\zeta_{m_4}}\times$$
$$\left.\times\,\mathrm{E}\left[\exp\left\{-j\left(\Phi^{(k_1)}_{2,m_1}(t)-\Phi^{(k_2)}_{2,m_2}(t)+\Phi^{(k_3)}_{3,m_3}(t+\tau)-\Phi^{(k_4)}_{3,m_4}(t+\tau)\right)\right\}\right]\right\} \tag{14}$$

Following an approach similar to that of Appendix in [29] and considering that the phase shift associated with each PMP is a zero mean process, the autocorrelation of the STAXT generated in a MCF with multiple excited cores is independent of the level of power splitting between the polarization directions, and can be approximated as:

$$R_{STAXT,n}(\tau) \approx \sum_{\substack{m=1,\\ m\neq n}}^{N_c} p^2_{i,m}|\overline{K}_{n,m}|^4\left[N_p^2+\frac{N_p}{2}(N_p-1)R^2_m(\tau)\right]+N_p^2\sum_{\substack{m_1=1,\\ m_1\neq n}}^{N_c}p_{i,m_1}|\overline{K}_{n,m_1}|^2\times$$
$$\times\sum_{\substack{m_2=1,\\ m_2\neq n,\\ m_2\neq m_1}}^{N_c}p_{i,m_2}|\overline{K}_{n,m_2}|^2+\frac{N_p^2}{2}\sum_{\substack{m_1=1,\\ m_1\neq n}}^{N_c}p_{i,m_1}|\overline{K}_{n,m_1}|^2R_{m_1}(\tau)\sum_{\substack{m_2=1,\\ m_2\neq n,\\ m_2\neq m_1}}^{N_c}p_{i,m_2}|\overline{K}_{n,m_2}|^2R_{m_2}(\tau) \tag{15}$$

Optics EXPRESS

where $R_l(\tau)$=$R_{ns,l}(\tau)$ whether the non-stationary phase shift model is considered. In the case of the stationary phase shift model, $R_l(\tau)$=exp $\left(-\sigma^2_{\Phi_l} + R_{\Phi_l}(\tau)\right)$ where the autocorrelation of each phase shift of the l-th interfering core is given by [29]:

$$R_{\Phi_l}(\tau) = \sigma^2_{\Phi_l} \exp(-\alpha_l|\tau|)(\cos(\alpha_l\tau) + \sin(\alpha_l|\tau|)) \tag{16}$$

$\sigma^2_{\Phi_l}$ is the variance of the phase shift and α_l is a parameter that enables adjusting the decorrelation time of the STAXT generated by core l [29]. The autocovariance of the STAXT of core n generated in a MCF with multiple excited cores can be obtained from the autocorrelation as:

$$C_{STAXT,n}(\tau) = R_{STAXT,n}(\tau) - \mathrm{E}^2[p(t)] \approx \frac{N_p(N_p-1)}{2} \sum_{\substack{m=1,\\ m\neq n}}^{N_c} p^2_{i,m}|\overline{K}_{n,m}|^4 R^2_m(\tau) +$$

$$+ \frac{N_p^2}{2} \sum_{\substack{m_1=1,\\ m_1\neq n}}^{N_c} p_{i,m_1}|\overline{K}_{n,m_1}|^2 R_{m_1}(\tau) \sum_{\substack{m_2=1,\\ m_2\neq n,\\ m_2\neq m_1}}^{N_c} p_{i,m_2}|\overline{K}_{n,m_2}|^2 R_{m_2}(\tau) \tag{17}$$

where we have considered the square of the mean STAXT power given by:

$$\mathrm{E}^2[p(t)] = N_p^2 \sum_{\substack{m=1,\\ m\neq n}}^{N_c} p^2_{i,m}|\overline{K}_{n,m}|^4 + N_p^2 \sum_{\substack{m_1=1,\\ m_1\neq n}}^{N_c} p_{i,m_1}|\overline{K}_{n,m_1}|^2 \sum_{\substack{m_2=1,\\ m_2\neq n,\\ m_2\neq m_1}}^{N_c} p_{i,m_2}|\overline{K}_{n,m_2}|^2 \tag{18}$$

Let us consider that the discrete coupling coefficients, the powers at the output of the fan-in for the different cores and the statistical properties of the phase shifts of the cores are identical. In this case, Eq. (17) can be simplified to:

$$C_{STAXT,n}(\tau) \approx (N_c-1)\left[\frac{N_p^2 - N_p}{2} + (N_c-2)\frac{N_p^2}{2}\right] p^2_{i,m}|\overline{K}_{n,m}|^4 R^2_m(\tau) \tag{19}$$

Equation (19) shows that, with the ICXT model given by Eq. (1), the time dependence of the STAXT autocovariance in MCFs with multiple excited cores is similar to that one obtained when only one interfering core is considered. Particularly, it can be concluded from Eq. (19) that the STAXT decorrelation time is the same regardless the number of interfering cores. This conclusion holds for cores with identical discrete coupling coefficients and statistical properties of the phase shifts and is somehow in conflict with the work reported in [17], where it is concluded that the decorrelation time of the STAXT becomes smaller when the number of interfering cores increases. We will detail this discussion later on this paper when validating our model with experimental results.

Let us consider also the case where the STAXT is generated by a single interfering core. In this case, the autocovariance of the STAXT induced by core m in core n is given by:

$$C_{STAXT,n}(\tau) \approx \frac{N_p(N_p-1)}{2} p^2_{i,m}|\overline{K}_{n,m}|^4 R^2_m(\tau) \tag{20}$$

If the non-stationary phase shift model is considered, $R^2_m(\tau) = \exp(-K_{\Phi_m}|\tau|)$ and, thus, K_{Φ_m}=$1/T_{STAXT,m}$ where $T_{STAXT,m}$ is the decorrelation time at $1/e$ of the STAXT generated by core m.

Optics EXPRESS

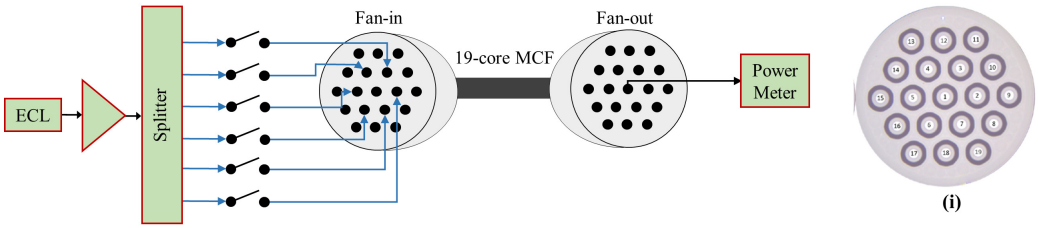

Fig. 1. Experimental setup implemented in the lab to measure the STAXT. (i) Profile of the 19-core MCF.

3. Experimental and simulation setup

Figure 1 depicts the schematic diagram of the experimental setup implemented in the lab to measure the STAXT. An external cavity laser (ECL) is used to generate the continuous wave signal and the optical amplifier is used to boost the optical power. The optical signals to be launched into each MCF core are obtained at the output of an optical splitter. The CW signals injected in the different MCF cores are generated by the same laser source. However, as the ICXT mechanism of the MCFs is an intrinsic effect of the fiber and does not depend on the light source, we do not expect to obtain different results/conclusions if different sources are used to generate the light to be injected in the different cores. The optical power at the input of the fan-in is 0 dBm for each core. The MCF is a 20 km-long homogeneous trench-assisted 19-core fiber with profile as shown in inset (i) of Fig. 1. The cladding diameter is 180 μm, the core pitch is 32 μm and the core diameter is 9 μm. The loss of the MCF in each core is 0.4-0.5 dB/km. In addition, three splices with loss per splice below 1 dB are located at 10.5 km, 11 km and 12.5 km. The total loss of the fan-in+MCF+fan-out for each core of the MCF used in this work is shown in Table 1. The loss of the fan-in+fan-out devices, including fans splicing, is below 5 dB. The STAXT is measured at the output of the central core (core 1) with two configurations of interfering cores: (i) with only one interfering core, in which the STAXT induced by cores 2 to 7 is assessed individually, and (ii) with six interfering cores, in which the optical signals are launched in cores 2 to 7 simultaneously. Note that the ICXT generated in the central core due to the outer cores (cores 8 to 19) of the MCF is negligible compared to the ICXT generated by cores 2 to 7. The STAXT at the output of the central core is monitored continuously over several days with experimental measurements taken with a time period of 2 seconds.

In addition to experimental measurements of the STAXT, simulation of the setup shown in Fig. 1 is also performed. In the simulation, the ICXT is generated using Eq. (1). This equation includes the effects of group velocity dispersion (dispersion parameter of each core is, approximately, 20 ps/nm/km) and skew between the pair of cores. The skew of the pair of cores under analysis in this work is shown in Table 2. The STAXT is evaluated over a time window of 10 hours and considering 1000 PMPs [13, 15, 29]. The number of PMPs is associated with the number of points along the longitudinal direction of the MCF in which the difference between the effective refractive indexes of the core of the originating signal and the core of ICXT is zero [31]. This

Table 1. Total fan-in+MCF+fan-out loss.

Cores	Loss [dB]	**Pair of cores**	Loss [dB]
(1)	14.2	**(5)**	15.3
(2)	17.3	**(6)**	14.2
(3)	14.6	**(7)**	16.2
(4)	14.5	-	-

Optics EXPRESS

number of PMPs is proportional to the MCF length [6, 12]. Therefore, it is expected that a higher number of PMPs is required when the MCF length increases. However, further investigation showed that, even for longer MCFs, adequate description of the ICXT statistics is obtained by simulation with 1000 PMPs as the mean, variance and autocorrelation function of the STAXT are almost the same as those ones achieved with a higher number of PMPs. This was confirmed considering the PMPs distributed uniformly or randomly along the fiber and for MCF lengths reaching 2000 km. In this work, the longitudinal coordinate of each PMP is calculated as follows: (i) the length of the MCF is divided in 1000 segments with equal length, and (ii) in each segment, the PMP coordinate follows an uniform distribution.

4. Simulation results

In this section, the analytical results of the autocorrelation and autocovariance of the STAXT evaluated from Eq. (15) and Eq. (17) for a MCF with multiple excited cores are validated by comparison with numerical simulation of Eq. (1). The same level of optical power is considered at the input of all interfering cores and identical MCF loss in the different cores is assumed.

Figure 2(a) and Fig. 2(b) depict the autocorrelation and autocovariance of the STAXT, respectively, at the output of the central core considering the stationary phase shift model. A MCF with six interfering cores characterized by a discrete coupling coefficient in each core of -78 dB is considered. Two different STAXT decorrelation time configurations are analyzed:

> Case 1: the STAXT decorrelation time of each pair of cores is 5 minutes. With the stationary phase shift model, this decorrelation time is obtained by setting α_l=7.19 $\times$ 10^{-4} s^{-1};
>
> Case 2: the STAXT decorrelation time is 2 minutes for pairs (1,2), (1,3) and (1,4), and 5 minutes for pairs (1,5), (1,6) and (1,7). In the case of the stationary phase shift model, the decorrelation time of 2 minutes is obtained by setting α_l=18 $\times$ 10^{-4} s^{-1}.

In addition, simulation results for different power splitting levels between the polarization directions at the input of each interfering core are shown in Fig. 2. Figure 2(c) and Fig. 2(d) show results similar to Fig. 2(a) and Fig. 2(b) but considering the non-stationary phase shift model. Figure 2 shows excellent agreement between the analytical and simulation results of the STAXT autocorrelation and autocovariance functions. This conclusion holds for the two phase shift models analyzed and confirms that the STAXT autocovariance and autocorrelation functions are independent from the fiber dispersion, skew between cores and power splitting levels between the polarization directions at the fiber input. As shown in Fig. 2(b) and Fig. 2(d), the decorrelation time evaluated at $1/e$ from the STAXT autocovariance function is 5 minutes (case 1) and 3 minutes (case 2) regardless the phase shift model considered. Two important conclusions can be drawn from these decorrelation time results. In a MCF with multiple interfering cores, if the different pairs of cores are characterized by identical discrete coupling coefficients and by phase shifts with identical statistical properties, the decorrelation time of the STAXT of the interfered core obtained with one or multiple interfering cores is the same, as indicated by Eq. (19). When the pairs of cores are characterized by different STAXT decorrelation times, the STAXT decorrelation time measured in the test core with multiple interfering cores is higher

Table 2. Skew between the pair of cores.

Pair of cores	Skew [ns]	**Pair of cores**	Skew [ns]
(1,2)	5.4	**(1,5)**	2.4
(1,3)	4.8	**(1,6)**	7.0
(1,4)	3.2	**(1,7)**	3.3

Optics EXPRESS

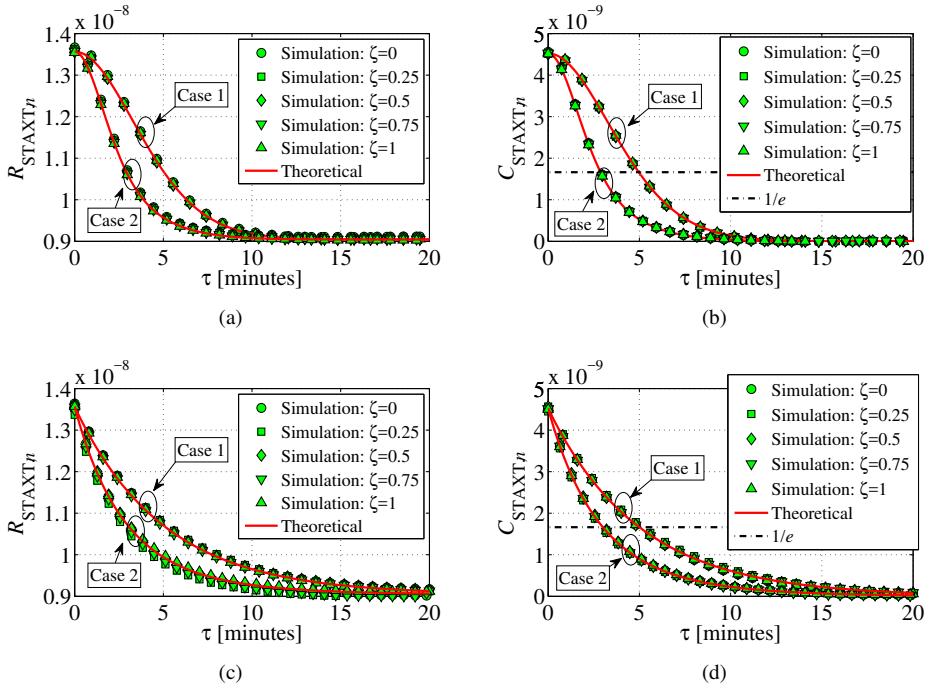

Fig. 2. (a) Autocorrelation and (b) autocovariance functions of the STAXT of the central core considering the stationary phase shift model. (c) Autocorrelation and (d) autocovariance functions of the STAXT of the central core considering the non-stationary phase shift model. The results are evaluated considering six interfering cores. Case 1: the STAXT decorrelation time of each pair of cores is 5 minutes. Case 2: the STAXT decorrelation time is 2 minutes for pairs (1,2), (1,3) and (1,4), and 5 minutes for pairs (1,5), (1,6) and (1,7).

than that one of the pair of cores with lower STAXT decorrelation time. This occurs because the ICXT power generated in the interfered core results from different contributions: one, that is faster and that corresponds to the cores with smaller decorrelation time, and other, slower, corresponding to the cores with larger decorrelation time. Thus, the resulting ICXT generated by multiple cores with faster and slower decorrelation times is characterized by random time fluctuations with intermediate decorrelation time.

5. Experimental results

In the following, the experimental results of the STAXT considering a MCF with a single interfering core and with six interfering cores are presented. From these results, the STAXT autocovariance evaluated from experimental measurements is obtained and compared with the STAXT autocovariance proposed in Eq. (17) for a MCF with multiple interfering cores. In addition, the theoretical decorrelation times of the STAXT are also compared with those ones estimated from experimental measurements with single and multiple interfering cores.

5.1. One interfering core

5.1.1. STAXT

Figure 3 depicts the STAXT measured in the central core over 160 hours for six different interfering cores. Power variations of the STAXT over time exceeding 20 dB can be observed. It

Optics EXPRESS

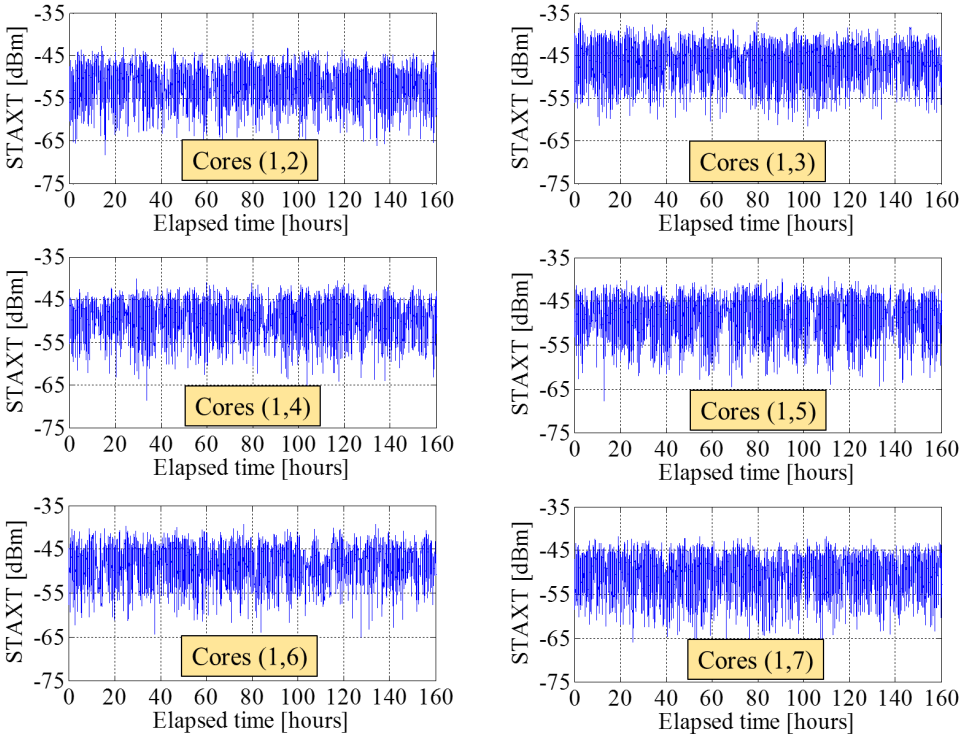

Fig. 3. STAXT of the central core measured over 160 hours for different interfering cores.

is also shown that the STAXT induced by core 3 in core 1 is higher than the STAXT generated by the other cores. The experimental results of the STAXT power at the output of the central core considering only one interfering core are useful to estimate the discrete coupling coefficient, $\overline{K}_{n,m}$, between core 1 and each one of the other interfering cores (2 to 7). This is achieved by evaluating the average ICXT power for each pair of cores shown in Fig. 3 over the 160 hours period and taking into account that, for ergodic processes, $N_p|\overline{K}_{n,m}|^2 \approx \frac{\overline{p}_{XT,n} a_{total,m}}{p_{in,m}} \frac{l_{f-o,n}}{l_{f-o,m}}$, where $a_{total,m}$ is the loss of fan-in+MCF+fan-out in core m, $l_{f-o,l}$ is the insertion loss of the fan-out associated with the l-th output, $\overline{p}_{XT,n}$ is the average ICXT power generated by core m at the output of the fan-out corresponding to core n and $p_{in,m}$ is the power at the input of the fan-in in the interfering core m, i e., $\frac{p_{in,m}}{p_{i,m}} = l_{f-i,m}$ where $l_{f-i,m}$ is the insertion loss of the fan-in associated with the m-th input. Table 3 shows the parameters used to estimate the discrete coupling coefficients from experimental measurements of the STAXT. Identical MCF loss in each core (0.5 dB/km and 2.5 dB for MCF splices), similar insertion loss for the fan-in and fan-out devices, and the total loss of the fan-in+MCF+fan-out shown in Table 1 are considered. In addition, 1000 PMPs are considered to evaluate the discrete coupling coefficients. Other number of PMPs could be used to estimate the discrete coupling coefficients from the average ICXT power measured experimentally as far as the same number of PMPs is used also to evaluate the autocovariance of the STAXT from the theoretical model proposed in section 2.2.

5.1.2. Autocovariance

Figure 4 depicts the autocovariance of the STAXT at the output of the central core considering core 2 or core 6 as the interfering core. Results obtained from experimental measurements and evaluated from Eq. (17) considering the stationary and non-stationary phase shift models are

Optics EXPRESS

Table 3. Parameters used to estimate the discrete coupling coefficients. The mean ICXT power measured experimentally is also shown.

Cores (*n*,*m*)	$\overline{p}_{XT,n}$ [dBm]	$l_{f-o,m}$ [dB]	$\overline{K}_{n,m}$ [dB]	$P_{i,m}$ [dBm]	E[$p(t)$] [dBm]
(1,1)	–	0.85	–	–	–
(1,2)	-50.3	2.40	-64.55	-2.40	-36.95
(1,3)	-45.2	1.05	-60.80	-1.05	-31.85
(1,4)	-48.0	1.00	-63.65	-1.00	-34.65
(1,5)	-46.9	1.40	-62.15	-1.40	-33.55
(1,6)	-46.9	0.85	-62.70	-0.85	-33.55
(1,7)	-48.8	1.85	-63.60	-1.85	-35.45

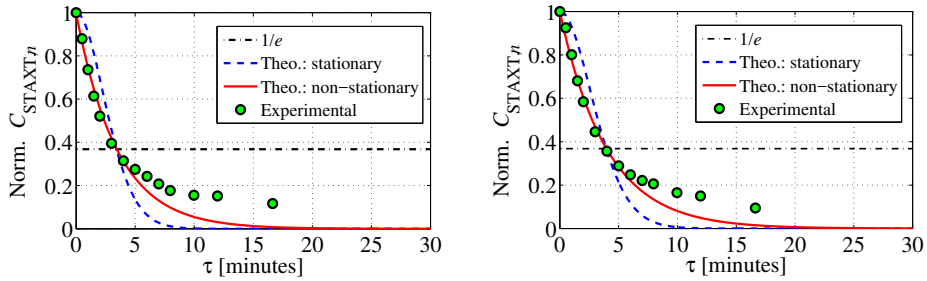

Fig. 4. Normalized autocovariance of the STAXT for the pair of cores (a) (1,2) and (b) (1,6).

presented. Very good agreement between the experimental results and the STAXT autocovariance evaluated from the dual polarization ICXT theoretical model with the phase shifts modeled by the non-stationary process is observed for most of the time lag values analyzed. Figure 4 shows that the autocovariance function evaluated from the stationary model is characterized by a decay that is much faster than the one measured experimentally. Instead, the decay of the autocovariance obtained with the non-stationary phase shift model and evaluated from experimental measurements is quite similar for the time lags with higher STAXT correlation. Some inconsistency between the experimental data and the non-stationary based theoretical results occurs in the tails of the autocovariance function. Currently, we are not completely sure of the origin of this inconsistency. However, we conceive that the inconsistency may result from (i) some inaccuracy of the experimental measurements, (ii) due to its simplicity, the model proposed is unable to completely characterize the mechanism associated with the random time variation of the ICXT in MCFs leading to some inaccuracy in the tails of the autocovariance of the STAXT and (iii) the contribution of the crosstalk induced by the fan-in and fan-out devices to the autocovariance of the STAXT may not be neglected in the tail region.

5.1.3. STAXT decorrelation time

The speed of the ICXT fluctuations is of special concern in MCF-based systems as it affects the design of ICXT-tolerant adaptive techniques and also how often the service is interrupted. The ICXT fluctuations can be characterized by the STAXT decorrelation time evaluated from the autocovariance function. The most common definition of decorrelation time is the decorrelation time evaluated at $1/e$ of the maximum of the autocovariance function [15, 29]. Previous work showed by simulation that an accurate estimation of the decorrelation time may require the continuous monitoring of the STAXT over a quite long time period [29]. In order to confirm

Optics EXPRESS

this conclusion experimentally, the STAXT generated in the central core by cores 2 to 7 was monitored individually in the lab over more than six consecutive days leading to a time period of accumulated measurements of more than one month. After capturing the STAXT measurements for each pair of cores, the autocovariance of the STAXT and, thus, the decorrelation time, were evaluated considering STAXT measurements obtained in time periods with different extensions.

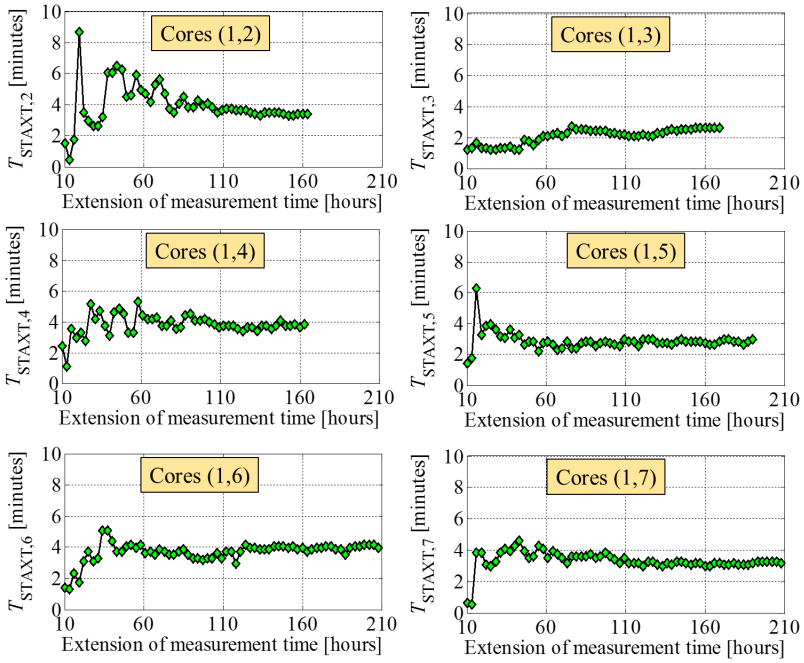

Fig. 5. Decorrelation time of the STAXT measured experimentally at the output of the central core as a function of the extension of the measurement time.

Figure 5 shows the decorrelation time of the STAXT measured experimentally at the output of the central core as a function of the time period extension over which the STAXT is monitored. Results for all the nearest neighboring cores are presented. Two main conclusions, valid for all pairs of cores under analysis, can be drawn from the inspection of Fig. 5. (i) The decorrelation time of the STAXT for the pair of cores under analysis is between 2 and 4 minutes. (ii) An extension of the measurement time of more than 100 hours may be required to get stabilized estimates of decorrelation times of the order of a few minutes. Even using a time window with extension of more than 100 hours, slight fluctuations of the decorrelation time when the extension of the measurement time increases are still observed. In order to reduce this fluctuation effect, we calculate the decorrelation time of each pair of cores as the average of the decorrelation times obtained for the last 30 hours of the measurement time extension shown in Fig. 5. These decorrelation times of the STAXT measured experimentally for each pair of cores are presented in Table 4.

5.2. Six interfering cores

5.2.1. STAXT

Figure 6(a) shows the STAXT measured in the central core when the optical power is injected simultaneously in the six adjacent cores. The comparison between Fig. 6(a) and Fig. 3 shows that, when the number of interfering cores increases, the STAXT power also increases, as expected. Figure 6(a) shows also fluctuations of the STAXT induced by the random time nature of the

Optics EXPRESS

Table 4. Decorrelation time of the STAXT measured experimentally at the output of the central core.

Pair of cores	T_{STAXT}	**Pair of cores**	T_{STAXT}
(1,2)	3.4 minutes	**(1,5)**	2.8 minutes
(1,3)	2.6 minutes	**(1,6)**	4.0 minutes
(1,4)	3.7 minutes	**(1,7)**	3.0 minutes

ICXT with magnitude exceeding 20 dB which is similar to the magnitude observed with only one interfering core.

5.2.2. Autocovariance

Figure 6(b) shows the normalized autocovariance of the STAXT measured experimentally and evaluated from Eq. (17) with the stationary and non-stationary phase shift models. The results are presented for six interfering cores. Very good agreement between the experimental results and the STAXT autocovariance model of Eq. (17) is observed when the non-stationary phase shift model is used. These results confirm the validity of the proposed model to describe the random time nature of the ICXT in weakly-coupled MCFs with multiple interfering cores.

5.2.3. STAXT decorrelation time

Figure 6(c) shows the experimental results of the decorrelation time of the STAXT of the central core when the six nearest neighboring cores are used as interfering cores. Figure 6(c) shows that

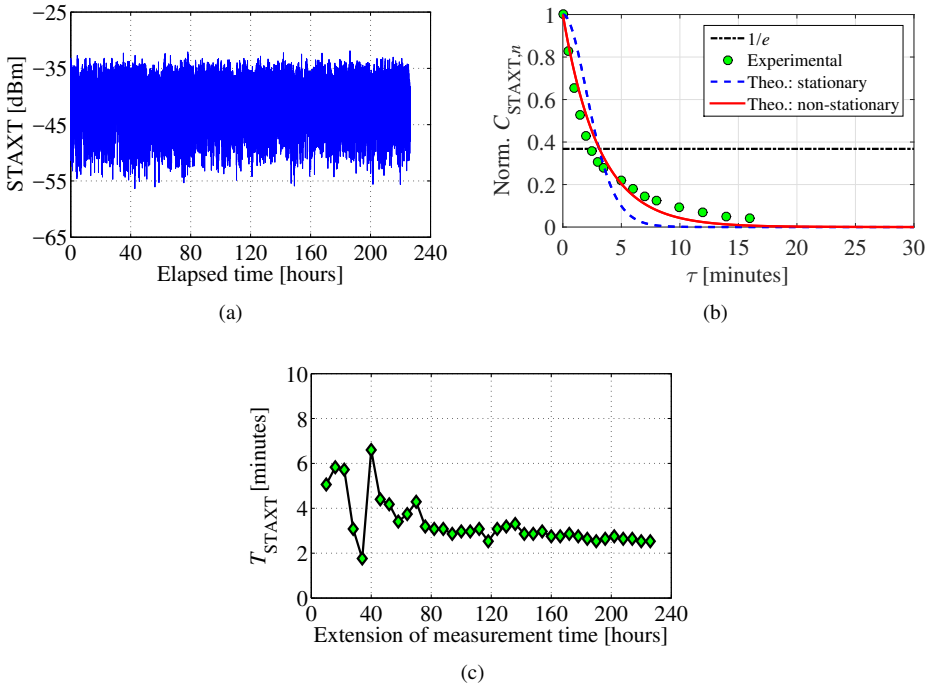

Fig. 6. (a) STAXT, (b) normalized autocovariance and (c) decorrelation time of the STAXT measured experimentally at the output of the central core. All the results are obtained considering six interfering cores.

Optics EXPRESS

stabilized estimates of the decorrelation time of the STAXT obtained with six interfering cores requires a measurement time extension of almost 200 hours. If we calculate the decorrelation time of each pair of cores as the average of the decorrelation times obtained for the last 30 hours of the measurement time extension shown in Fig. 6(c), the decorrelation time of the STAXT evaluated experimentally with six interfering cores is 2.7 minutes which is of the same order of magnitude of the decorrelation time of the STAXT obtained for each pair of cores, as predicted by Eq. (17). Using, for each pair of cores, the decorrelation times of the STAXT presented in Table 4 and the coupling coefficients of Table 3, the decorrelation time of the STAXT, evaluated from the autocovariance function given by Eq. (17) with six interfering cores, is 3 minutes which agrees quite well with the experimental data.

The work presented in [17] concluded that the decorrelation time of the STAXT is smaller when the number of interfering cores increases. Unfortunately, only the time evolution of the STAXT and the final STAXT decorrelation time values are shown in [17]. Information concerning the autocovariance function, from which the decorrelation times are evaluated, or the evolution of the decorrelation time as a function of the extension of the time measurement of the STAXT are not provided. However, there is an interesting point when comparing the results of [17] with those ones presented above. We concluded from Fig. 5 and Fig. 6(c) that more than 100 hours of STAXT measurements are required to get stabilized estimates of the decorrelation time obtained from experimental results. Despite the decorrelation times of each pair of cores involved in this work and in [17] are of the same order of magnitude (couple of minutes), the calculations of the decorrelation time performed in [17] use STAXT measurements taken only over 6 hours. From our experience, this seems a quite short time interval to get stabilized and accurate decorrelation time estimates, and can lead to misleading conclusions.

6. Conclusion

We have proposed, for the first time, a simple channel model to emulate the stochastic time evolution of the ICXT in homogeneous weakly-coupled MCFs with multiple interfering cores. Instead of using stationary phase shifts between consecutive PMPs as considered in a previous work, the proposed model relies on the introduction of non-stationary phase shifts. Very good agreement between the autocovariance of the STAXT evaluated from the proposed ICXT model and from experimental results taken over long time measurements (more than 150 hours) has been shown for MCFs with single and multiple interfering cores. Experimental results showed that the fluctuations of the STAXT induced by multiple interfering cores are characterized by a decorrelation time that exceeds the one of the pair of cores with shorter decorrelation time. A decorrelation time of 2.7 minutes for the STAXT generated by six interfering cores has been obtained experimentally with a measurement time period of 200 hours. The proposed ICXT model provides a decorrelation time of the STAXT generated by the six interfering cores of 3 minutes considering a decorrelation time of the STAXT measured experimentally for each pair of cores between 2.6 and 4 minutes. With this simple stochastic ICXT model, ICXT properties can be accurately emulated and the design of MCF systems can be increasingly pursued.

Funding

Fundação para a Ciência e a Tecnologia (FCT) (AMEN-UID/EEA/50008/2013, IF/01225/2015/CP1310/CT0001); Instituto de Telecomunicações (AMEN-UID/EEA/50008/2013).